environmental microbiology

Environmental Microbiology (2020) **22**(12), 5373–5386 doi:10.1111/1462-2920.15266

FgPal1 regulates morphogenesis and pathogenesis in *Fusarium graminearum*

Jinrong Yin,[1†] Chaofeng Hao,[1†] Gang Niu,[1] Wei Wang,[1] Guanghui Wang,[1] Ping Xiang,[1] Jin-Rong Xu [2] and Xue Zhang [1*]

[1]*State Key Laboratory of Crop Stress Biology for Arid Areas, College of Plant Protection, Northwest A&F University, Yangling, Shaanxi, 712100, China.*

[2]*Department of Botany and Plant Pathology, Purdue University, West Lafayette, IN, 47907.*

Summary

Ascospores are the primary inoculum in *Fusarium graminearum*, a causal agent of wheat head blight. In a previous study, *FgPAL1* was found to be upregulated in the *Fgama1* mutant and important for ascosporogenesis. However, the biological function of this well-conserved gene in filamentous ascomycetes is not clear. In this study, we characterized its functions in growth, differentiation and pathogenesis. The *Fgpal1* mutant had severe growth defects and often displayed abnormal hyphal tips. It was defective in infectious growth in rachis tissues and spreading in wheat heads. The *Fgpal1* mutant produced conidia with fewer septa and more nuclei per compartment than the wild type. In actively growing hyphal tips, FgPal1-GFP mainly localized to the subapical collar and septa. The FgPal1 and LifeAct partially co-localized at the subapical region in an interdependent manner. The *Fgpal1* mutant was normal in meiosis with eight nuclei in developing asci but most asci were aborted. Taken together, our results showed that FgPal1 plays a role in maintaining polarized tip growth and coordination between nuclear division and cytokinesis, and it is also important for infectious growth and developments of ascospores by the free cell formation process.

Received 20 February, 2020; accepted 29 September, 2020. *For correspondence. E-mail xuezhang@nwafu.edu; Tel. 13201577924. †These authors have contributed equally to this work.

Introduction

The homothallic filamentous ascomycete *Fusarium graminearum* is a causative agent of Fusarium head blight (FHB) or scab of wheat worldwide (Bai and Shaner, 2004; Zhang *et al*., 2012). It also infects barley, corn and other grain crops. Ascospores forcibly released from perithecia formed on plant debris are the primary inoculum of this important pathogen (Markell and Francl, 2003). Plant infection is initiated when airborne ascospores land on flowering wheat heads, germinate and penetrate plant cells directly or with specialized infection structures including infection cushions and lobate appressoria (Boenisch and Schäfer, 2011; Jiang *et al*., 2019). Infectious growth is then spread from infected kernels to other spikelets on the same wheat head via the rachis and cause head blight symptoms. Under favourable environmental conditions, *F. graminearum* can cause severe yield losses and contaminate infested grains with mycotoxins such as deoxynivalenol (DON) and zearalenone (Trail *et al*., 2002; Goswami and Kistler, 2004). The trichothecene mycotoxin DON is a potent protein synthesis inhibitor in eukaryotic organisms and an important virulence factor in *F. graminearum* (Van de Walle *et al*., 2010).

Because of the role of ascospores as the primary inoculum, sexual reproduction is a critical step in the infection cycle of *F. graminearum*. As a homothallic fungus, it produces abundant perithecia by selfing on mating cultures in the laboratory or infected plant debris in the field (Miedaner *et al*., 2008; Kim *et al*., 2015). Mature perithecia are melanized and contain asci with eight four-celled ascospores. In each developing ascus, the diploid nucleus formed after karyogamy goes through meiosis and one round of post-meiotic mitosis before the delimitation of eight ascospores (Nakayashiki, 2005; Hao *et al*., 2019). The nucleus in each developing ascospores then undergoes two more rounds of mitosis and cytokinesis before the formation of four-celled ascospores with one nucleus per compartment. Repeat-induced point (RIP) mutation, meiotic silencing of unpaired DNA (MSUD) and A-to-I RNA editing are known to specifically occur in *F. graminearum* during sexual reproduction (Son *et al*., 2011; Hane *et al*., 2015; Liu *et al*., 2016). Although

RIP is a premeiotic event, MSUD occurs during meiosis or post-meiotic mitosis. Genome-wide A-to-I RNA editing has been shown to occur in mating cultures as early as 1 day post-fertilization (dpf) and increases during ascus development and ascospore formation (Liu *et al*., 2016; Teichert *et al*., 2017; Bian *et al*., 2019). Interestingly, 70 genes have premature stop codons (PSCs) that require A-to-I editing to encode full-length functional proteins in *F. graminearum*. Several genes with PSC editing events are known to be important for ascospore formation or release, including *PUK1*, *AMD1* and *FgAMA1* (Liu *et al*., 2016; Cao *et al*., 2017; Hao *et al*., 2019).

Unlike other mutants with defects in ascospore formation, the *Fgama1* mutant produced rounded ascospores that may grow by budding inside asci before being released from perithecia (Hao *et al*., 2019). *AMA1* is a meiosis-specific co-activator of the anaphase-promoting complex/cyclosome (APC/C) in the budding yeast *Saccharomyces cerevisiae* (Cooper *et al*., 2000). The *Fgama1* mutant is normal in meiosis and still produces eight ascospores in each ascus although it has abnormal ascospore morphology and ascospore budding defects. The *Fgama1* ascospores are one-celled but have two nuclei in each ascospore, indicating that *FgAMA1* is essential for cytokinesis and second round of mitosis in developing ascospores. RNA-seq analysis showed that one of the genes affected by *FgAMA1* deletion is the *FgPAL1* gene, which also has one PSC RNA editing event (Hao *et al*., 2019). Interestingly, the *Fgpal1* deletion mutant also has the ascospore budding defect and forms ascospores with abnormal morphology. However, unlike the *Fgama1* mutant, the *Fgpal1* mutant had severe defects in ascosporogenesis and rarely formed ascospores (Hao *et al*., 2019).

FgPal1 is orthologous to Pal1 of *S. cerevisiae* and *Schizosaccharomyces pombe* (Ge *et al*., 2005; Carroll *et al*., 2012). Pal1 is a membrane-associated protein that is involved in the maintenance of cylindrical cellular morphology although its exact function is not clear in the budding and fission yeasts. It localizes to the sites of active growth in *S. cerevisiae* and *S. pombe* (Ge *et al*., 2005). In *S. cerevisiae*, the *pal1* mutant (pears and lemons) forms yeast cells with morphology defects. Pal1 is an early-arriving endocytic coat protein recruited by Ede1 and the intermediate coat module protein Sla2, and it disassembles from endocytic sites before actin polymerization (Carroll *et al*., 2012). In *S. pombe*, Pal1 also physically interacts and partially co-localizes with Sla2, Ede1 and Syp1 at the endocytic site (Ge *et al*., 2005). Protein kinase Pom1, a member of the dual-specificity DYRK kinase family, directly phosphorylates Pal1 and other cell polarity targets to regulate cell polarity and cell cycle signalling (Kettenbach *et al*., 2015). Pal1 is also directly phosphorylated at distinct residues by the MARK/PAR-1 protein kinase Kin1, which affects the localization of Pal1 to the growing cell ends of *S. pombe* (Lee *et al*., 2018).

Although there are only limited studies on the localization and functions of Pal1 in the budding and fission yeasts, its orthologues are well conserved in filamentous ascomycetes. However, the biological functions of Pa1l orthologues have not been studied in filamentous or plant pathogenic fungi. In this study, we further characterized its functions in hyphal growth, conidiation, sexual reproduction and pathogenesis in *F. graminearum*. The *Fgpal1* mutant was significantly reduced in growth rate and formed apical or subapical swollen bodies in growing hyphae. It also produced conidia with morphological defects and was defective in infectious growth in rachis tissues for disease spreading. In comparison with the wild type, the number of nuclei in each compartment was increased in the *Fgpal1* mutant. FgPal1-GFP mainly localized to the subapical collar and septa in an F-actin dependent manner and deletion of *FgPAL1* affected the localization of F-actin at the subapical region. FgPal1 played a role in both general endocytosis and clathrin-mediated endocytosis (CME) by disturbing the localization of FgEde1. During sexual reproduction, the *Fgpal1* mutant was normal in meiosis and formation of eight nuclei in developing asci but most of mutant asci were aborted in ascospore formation and rarely formed ascospores. Overall, our results showed that FgPal1 plays a role in maintaining normal hyphal growth, tip morphology and coordination between nuclear division and cytokinesis, and it is also important for infectious growth and developments of ascospores by the free cell formation process. The function of FgPal1 orthologues in the control of polarized growth and spatial regulation of cytokinesis may be conserved in other filamentous ascomycetes.

Results

FgPal1 is important for normal tip growth

In a previous study, *FgPAL1* (FGSG_08726) was found to be upregulated in the *Fgama1* mutant and important for ascosporogenesis (Hao *et al*., 2019). *FgPAL1* is orthologous to *PAL1* of *S. cerevisiae* and encodes a 521 amino acid (aa) protein with a conserved PAL1 domain at the C-terminal region. However, FgPal1 has an FtsK domain (55–172 aa) that is absent in its orthologues in *S. cerevisiae* and *S. pombe* (Fig. 1A). The FtsK domain first identified in bacteria is related to the translocation of DNA prior to the completion of cytokinesis and cell division (Steiner *et al*., 1999). Interestingly, the FtsK domain is well conserved in the FgPal1 orthologues in filamentous ascomycetes although none of them has been functionally characterized. Because the

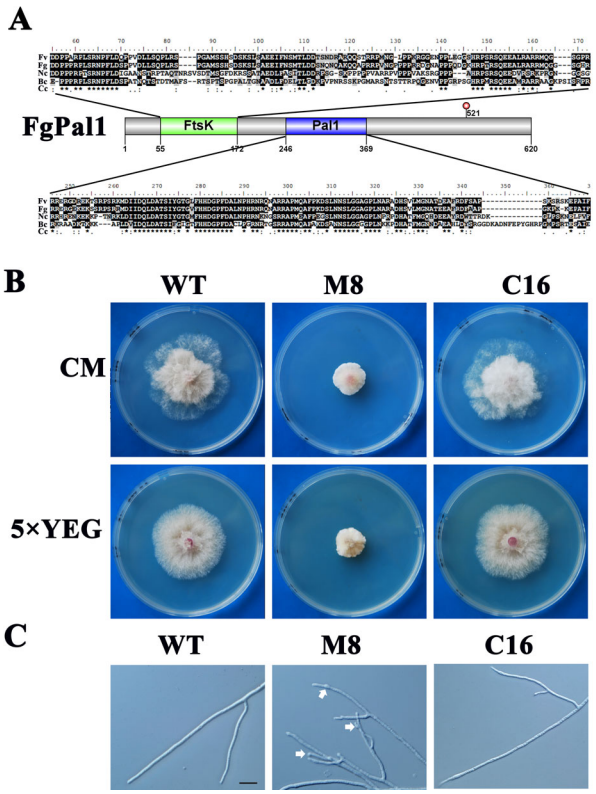

Fig. 1. Domain structure of FgPal1 and growth defects of the *Fgpal1* mutant. A. Schematic drawing of the conserved domains in FgPal1. The FtsK and Pal1 domains are shaded in green and blue respectively. The red circle marks the PSC subjected to A-to-I editing. Sequence alignment of FgPal1 and its orthologues from *Fusarium verticillioides* (Fv), *Neurospora crassa* (Nc), *Botrytis cinerea* (Bc), Clustal consensus (Cc) with the identical (*) or similar (·) amino acid residues marked. B. Three-day-old CM and 5× YEG cultures of the wild type (PH-1), *Fgpal1* mutant (M8) and complemented transformant (C16). C. CM cultures of PH-1, M8 and C16 were examined for hyphal tip growth and branching. Arrows point to apical or subapical swelling. Bar = 20 μm. [Color figure can be viewed at wileyonlinelibrary.com]

Table 1. Wild-type and mutant strains of *Fusarium graminearum* used in this study.

Strains	Brief descriptions	References
PH-1	Wild-type	Cuomo *et al*. (2007)
P8	*Fgpal1* deletion mutant of PH-1	Hao *et al*. (2019)
K1	*Fgkin1* deletion mutant of PH-1	Luo *et al*. (2014)
P1	*Fgpom1* deletion mutant of PH-1	Wang *et al*., (2011)
M8	*Fgpal1* deletion mutant of PH-1	This study
M9	*Fgpal1* deletion mutant of PH-1	This study
C6	*Fgpal1*/*FgPAL1*-GFP transformant of M8[a]	This study
C16	*Fgpal1*/*FgPAL1*-GFP transformant of M8	This study
PK1	*FgPAL1*-GFP transformant of K1	This study
PP1	*FgPAL1*-GFP transformant of P1	This study
PP4	*FgPAL1*-GFP transformant of P1	This study
PA1	LifeAct-RFP transformant of PH-1	This study
MA1	LifeAct-RFP transformant of M8	This study
PL6	*FgPAL1*-GFP transformant of PA1	This study
PL21	*FgPAL1*-GFP transformant of PA-1	This study
PH1-H	H1-GFP transformant of PH-1	This study
MH1-H	H1-GFP transformant of M8	This study
PS1	*FgSPA2*-GFP transformant of PH-1	This study
MS1	*FgSPA2*-GFP transformant of M8	This study
PAG1	LifeAct-GFP transformant of PH-1	This study
MAG1	LifeAct-GFP transformant of M8	This study
F7	$FgPAL1^{\Delta FtsK}$ in M8	This study
F8	$FgPAL1^{\Delta FtsK}$ in M8	This study
P3	$FgPAL1^{\Delta PAL1}$ in M8	This study
P5	$FgPAL1^{\Delta PAL}$ in M8	This study
PE1	*FgEDE1*-GFP transformant of PH-1	This study
ME1	*FgEDE1*-GFP transformant of M8	This study

[a]All the GFP and RFP fusion constructs were integrated ectopically in the genome.

previous study only identified one mutant strain and lacked complementation assays (Hao *et al*., 2019), in this study we first generated two additional *Fgpal1* mutants M8 and M9 (Table 1). All the *Fgpal1* mutant strains had similar defects described below although only data related to mutant M8 were presented.

The *Fgpal1* mutant was significantly reduced in growth rate in comparison with the wild-type strain PH-1 on complete medium (CM) and 5 × YEG (Fig. 1B; Table 2). It formed whitish, compact colonies that had more fluffy aerial hyphae than PH-1. Close examination of hyphal tips revealed that the *Fgpal1* mutant had defects in maintaining polarized tip growth and often had apical or subapical swollen bodies. Hyphae of the *Fgpal1* mutant appeared to have shorter distances between two branching sites, which might be related to its reduced growth rate (Fig. 1C). On average, the distance between two branching sites on growing hyphae was 79.5 ± 44.7 μm in the *Fgpal1* mutant, which was significantly shorter than that of the wild type (180.4 ± 78.5 μm). When the *FgPAL1*-GFP construct was transformed into the *Fgpal1* mutant, the resulting *Fgpal1*/*FgPAL1*-GFP transformants (Table 1) were normal in growth rate (Fig. 1B) and hyphal branching (Fig. 1C), indicating that the growth defects of *Fgpal1* mutant were directly related to the gene replacement event. Therefore, *FgPAL1* is important for hyphal growth, possibly by playing a role in maintaining normal polarized growth at the tip.

Because the *Fgpal1* and *Fgama1* mutants had similar defects in ascospore budding and *FgPAL1* expression was affected in *Fgama1*, we assayed their interaction by yeast two-hybrid assays. Yeast cells expressing the FgAma1 bait and FgPal1 prey constructs failed to grow on SD-Trp plates and had no LacZ activities (Fig. S1), indicating that FgPal1 and FgAma1 do not directly interact with each other.

To determine the effect of *FgPAL1* deletion on the polarisome or vesicle supply center at hyphal tips, we transformed the *FgSPA2*-GFP construct (Zhang *et al*., 2019) into PH-1 and the *Fgpal1* mutant M8. FgSpa2, a marker

Table 2. Defects of the *Fgpal1* mutant in growth, conidiation plant infection.

Strain	Growth rate (mm/day)[a]		Conidiation(10^5 spores ml^{-1})[b]	Disease index[c]
	CM	5 × YEG		
PH-1	8.9 ± 0.2^A	7.4 ± 0.4^A	15.2 ± 1.6^A	8.7 ± 1.7^A
M8	3.4 ± 0.0^B	3.2 ± 0.1^B	11.3 ± 1.7^B	1.0 ± 0.0^B
C16	8.7 ± 0.0^A	6.9 ± 0.1^A	14.5 ± 1.8^A	8.4 ± 1.5^A

Means ± SE were calculated from the results of three independent experiments. At least 10 wheat heads were examined in each repeat. Data were analysed with Duncan's pairwise comparison. Different letters mark statistically significant differences (p = 0.05).
[a]Growth rate was measured as the average daily expansion of colony radius after incubation on CM for 3 days.
[b]Number of conidia per ml in 5-day-old CMC cultures.
[c]Disease index was rated as the number of diseased spikelets per head at 14 dpi.

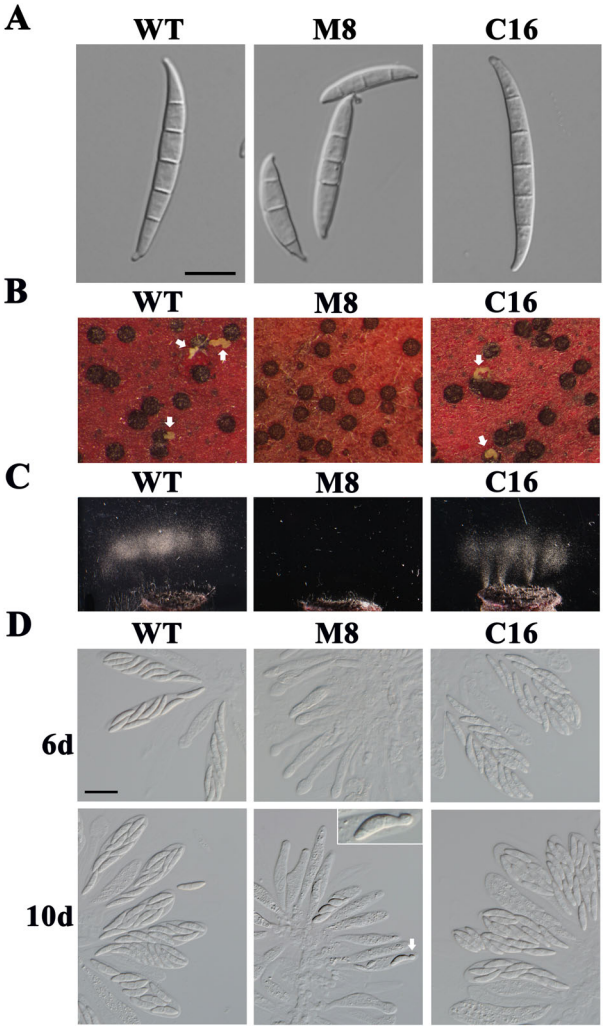

Fig. 2. Defects of the *Fgpal1* mutant in conidium morphology and sexual reproduction. A. Conidia produced by PH-1 (WT), *Fgpal1* mutants (M8) and *Fgpal1*/*FgPAL1-GFP* complemented transformant (C16) in CMC cultures. Bar = 10 μm. B. Two-week-old mating cultures were examined for perithecium formation and ascospore cirrhi (marked with arrows). C. Ascospore discharge was assayed with perithecia of the same set of strains collected at 7 dpf. D. Asci and ascospores formed by PH-1, mutant M8 and complemented strain C16. The inlet is a close-up view of the budding ascospore in mutant M8. Bar = 10 μm. [Color figure can be viewed at wileyonlinelibrary.com]

for the polarisome, is orthologous to Spa2, a cell polarity protein in *S. cerevisiae* (Takeshita and Fischer, 2019). In comparison with the wild type, the localization of FgSpa2-GFP was not affected in the *Fgpal1* mutant, indicating that FgPal1 is not involved in the localization of FgSpa2 to the hyphal tip (Fig. S2).

The Fgpal1 *mutant is defective in conidiation and sexual reproduction*

Similar to its reduced growth rate, the *Fgpal1* mutant was reduced in conidiation compared with the wild type in 5-day-old carboxymethyl cellulose (CMC) cultures (Table 2). Furthermore, conidia of the *Fgpal1* mutant (39.6 ± 6.4 μm in length) were shorter than those of the wild type (45.2 ± 7.9 μm in length) (Fig. 2A). Instead of forming typical 4–6 celled macroconidia, approximately 90% of *Fgpal1* conidia had three or fewer unevenly distributed septa. On average, conidia of the *Fgpal1* mutant had 3.1 ± 0.2 septa but the wild type had 4.3 ± 0.5 septa per conidium. However, conidium germination was normal in the *Fgpal1* mutant.

On mating cultures, the *Fgpal1* mutant still formed melanized perithecia but ascospore cirrhi were never observed (Fig. 2B) at 14 days post-fertilization (dpf) or even longer. In ascospore ejection assays, masses of ascospores were physically released from wild-type perithecia but not from *Fgpal1* perithecia (Fig. 2C). When examined for asci and ascospores inside perithecia, most of the wild-type asci were fertile and had eight ascospores per ascus (Fig. 2D). However, majority of the *Fgpal1* asci appeared to be aborted in ascospore formation and had granular cytoplasm. For the *Fgpal1* asci with ascospores, most of them had fewer than four ascospores per ascus and displayed ascospore morphology defects (Fig. 2D). These results further indicate that *FgPAL1* is dispensable for ascus development but important for ascospore formation and essential for ascospore release in *F. graminearum*.

FgPal1 is important for plant infection

In infection assays with flowering wheat heads of susceptible wheat cultivar Xiaoyan 22, the *Fgpal1* mutant only caused scab symptoms on the inoculated florets at 14 days post-inoculation (dpi) and failed to infect neighbouring spikelets on the same head. Under the same condition, the wild-type strain PH-1 developed typical head blight symptoms on the inoculated and neighbouring spikelets (Fig. 3A). In infection assays with corn silks, the *Fgpal1* mutant caused only limited discoloration at the inoculation site (Fig. 3B), confirming that *FgPAL1* is important for virulence in *F. graminearum*.

The *Fgpal1* mutant was similar to the wild type in the penetration of wheat lemma and development of invasive hyphae in infected lemma tissues at 48 hpi (Fig. 3C). Because the *Fgpal1* mutant was defective in spreading to neighbouring spikelets, we examined infectious growth in the rachis tissues. At 120 hpi, PH-1 produced extensive infectious hyphae in rachis tissues adjacent to the inoculated spikelet. However, in wheat heads inoculated with the *Fgpal1* mutant, we failed to observe invasive hyphae in rachis tissues below or above the inoculated spikelet (Fig. 3D). Therefore, *FgPAL1* must be essential for infectious hyphae to spread from inoculated florets through the rachis to other spikelets.

Because DON is an important virulence factor in *F. graminearum*, we also assayed DON production in infected wheat kernels (Li *et al*., 2015). In comparison with the wild type (3564.2 ± 312.0 ppm), the *Fgpal1* mutant was significantly reduced in DON production (1212.9 ± 193.0 ppm). These results suggest that deletion of *FgPAL1* affects DON biosynthesis during infection.

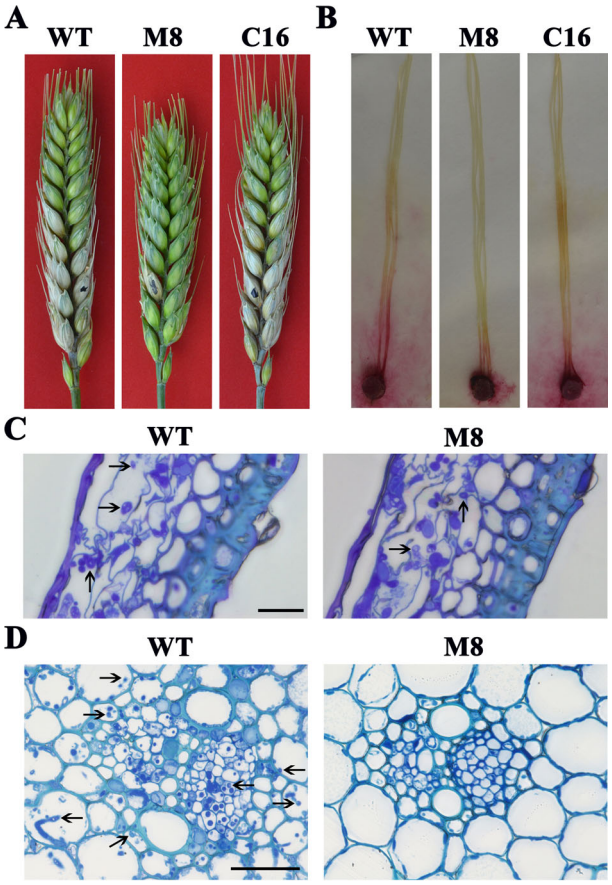

Fig. 3. Defects of the *Fgpal1* mutant in plant infection. A. Flowering wheat heads inoculated with the wild type (PH-1), *Fgpal1* mutants (M8) and complemented transformant (C16) were photographed at 14 dpi. Black dots marked the inoculation sites. B. Corn silks inoculated with the same set of strains were photographed at 5 dpi. C. Thick sections of wheat lemma inoculated with PH-1 and the *Fgpal1* mutant were stained with 0.5% (wt./vol.) toluidine blue and examined for infectious growth at 48 hpi. D. Thick sections of the rachis tissues right below the inoculated spikelets were examined at 120 hpi. For (C) and (D), invasive hyphae were marked with arrows. Bar = 20 μm. [Color figure can be viewed at wileyonlinelibrary.com]

FgPal1 localizes to the subapical collar region

In both *S. cerevisiae* and *S. pombe*, Pal1 localizes to the growing cell end at the interphase and affects cell morphology (Ge *et al*., 2005; Carroll *et al*., 2012). When hyphal tips or germ tube tips of the *Fgpal1*/*FgPAL1*-GFP transformant were examined, FgPal1-GFP signals were mainly observed at the subapical collar (Fig. 4A). Nevertheless, a few spots with bright GFP signals with dynamic locations also were observed in the cytoplasm in the region behind the hyphal tip (Fig. 4A), which may be related to the localization of FgPal1-GFP to developing septa.

To further characterize its subcellular localization, we co-transformed the *FgPAL1*-GFP construct with the LifeAct-RFP construct (Zhang *et al*., 2019) into the *Fgpal1* mutant M8. In the resulting transformants, LifeAct, an F-actin marker, localized to the tip apex (the polarisome) and collar region as being reported in other fungi (Delgado-Álvarez *et al*., 2010; Zhou *et al*., 2012). Unlike LifeAct-RFP signals, FgPal1-GFP signals were never observed at the tip apex. However, partial colocalization of FgPal1-GFP with LifeAct-FRP was observed in the sub-apical collar region (Fig. 4B). Besides the overlapping zone, FgPal1-GFP signals were on the side towards the tip and LifeAct-RFP signals were on the other side towards the rear end (Fig. 4B). The distribution of LifeAct-RFP and FgPal1-GFP signals may reflect their dynamic spatio-temporal association at the sub-apical collar.

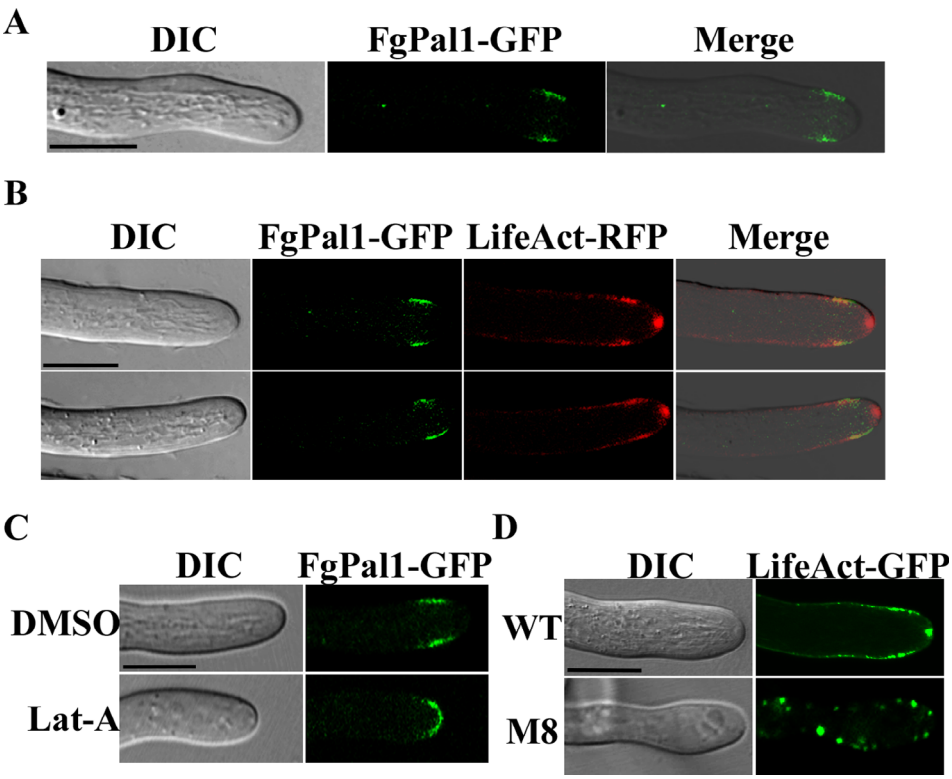

Fig. 4. Localization of FgPal1-GFP to the subapical region. A. Hyphal tips of the *Fgpal1*/*FgPAL1*-GFP transformant were examined for GFP signals after incubation in the SYM medium for 12 h. Bar = 10 μm. B. Germ tubes of the *FgPAL1*-GFP LifeAct-RFP transformant were examined by co-focal microscopy. Partial co-localization of FgPal1 and LifeAct was observed at the sub-apical collar region of actively growing hyphae. Bar = 20 μm. C. Vegetative hyphae of the *Fgpal1*/*FgPAL1*-GFP transformant were treated with Lat-A for 10 min and examined by epifluorescence microscopy. Bar = 20 μm. D. Hyphae of the *Fgpal1*/LifeAct-RFP and PH-1/LifeAct-RFP transformant were examined by epifluorescence microscopy. Bar = 20 μm. [Color figure can be viewed at wileyonlinelibrary.com]

The localization of FgPal1 to the collar region is dependent on F-actin and vice versa

Because of the partial co-localization of FgPal1 with F-actin, we treated the *Fgpal1*/*FgPAL1*-GFP transformant with Latrunculin A (Lat-A), an inhibitor of F-actin (Ge *et al*., 2005). After treating vegetative hyphae of the *Fgpal1*/*FgPAL1*-GFP transformant with 0.1 μg ml^{-1} Lat-A dissolved in dimethylsulfoxide (DMSO) for10 min, FgPal1-GFP signals localized to the apex of hyphal tips (Fig. 4C). In the control treated with DMSO along, FgPal1-GFP signals were still mainly at the sub-apical collar region. These results suggested that the localization of FgPal1-GFP to hyphal tips is F-actin dependent.

We then transformed the LifeAct-GFP construct (Delgado-Álvarez *et al*., 2010; Zhou *et al*., 2012) into the *Fgpal1* mutant. In the resulting *Fgpal1* LifeAct-GFP transformant, the LifeAct-GFP signals were observed only at the sub-apical collar region and some spots in the back where septation may initiate (Fig. 4D). In the wild type, LifeAct-GFP localized to the tip apex (the polarisome) and collar region (Fig. 4D). These results indicated that FgPal1 also played a role in the localization of LifeAct at hyphal tips, which further proved the dynamic association of FgPal1 and LifeAct at the sub-apical collar.

Deletion of FgPAL1 *affects the general endocytosis and CME*

In *A. nidulans* and *N. crassa*, actin patches in the subapical collar are sites for the occurrence of endocytosis, a process that plays an important role in polarized tip growth in filamentous fungi (Fischer-Parton *et al*., 2000; Araujo-Bazán *et al*., 2008). To test whether FgPal1 plays a role in endocytosis in *F. graminearum*, we compared the efficiency of the wild type (PH-1) and *Fgpal1* mutant in the uptake of FM4-64, a fluorescent dye commonly used as an endocytic marker or a tracer for endocytosis (Fischer-Parton *et al*., 2000). In the wild type, the plasma membrane and cytoplasm were quickly stained by FM4–64 in 10 min and vacuoles became visible by 30 min when FM4-64 was gradually internalized. In the *Fgpal1* mutant, FM4-64 appeared at the plasma membrane at 10 min but only weak fluorescent signals were visible in the cytoplasm by 30 min (Fig. 5A). These results suggested that FgPal1 is involved in both the uptake and general endocytosis of the fluorescent dye FM4-64.

Ede1 is an endocytic scaffolding protein involved in CME and it is important for endocytic site initiation and stabilization (Brach *et al*., 2014; Lu and Drubin, 2017). To further characterize the role of *FgPAL1* in endocytosis,

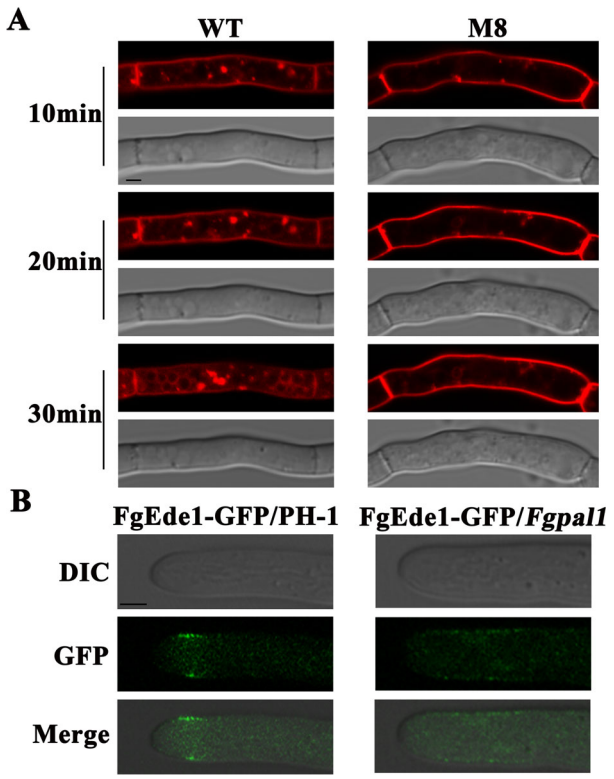

Fig. 5. Defects of the *Fgpal1* mutant in endocytosis. A. Hyphae of the wild type (PH-1) and *Fgpal1* mutants (M8) were stained with FM4-64 for 10, 20, or 30 min before being examined by epifluorescence microscopy. Bar = 10 μm. B. Hyphal tips of the *Fgpal1*/Ede1-GFP and PH-1/Ede1-GFP transformants were examined by epifluorescence microscopy. Bar = 10 μm. [Color figure can be viewed at wileyonlinelibrary.com]

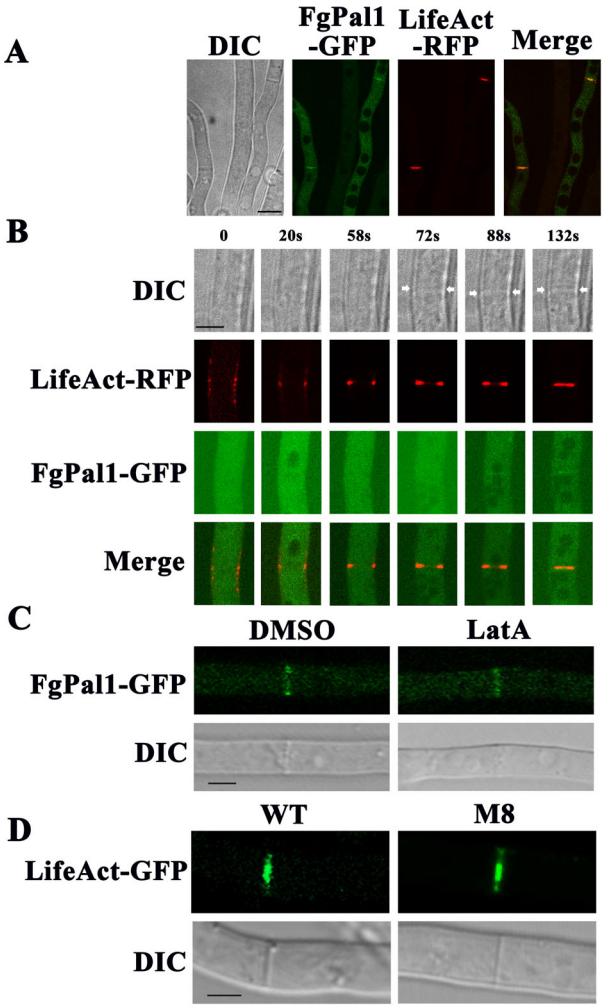

Fig. 6. Co-localization of FgPal1-GFP and LifeAct-RFP to the septum. A. Hyphae of the *FgPAL1*-GFP and LifeAct-RFP transformant PL1 were examined by epifluorescence microscopy. Bar = 20 μm. B. A time-course (0–132 s) to show the co-localization of LifeAct and FgPal1 during septum formation. Bar = 20 μm. C. Vegetative hyphae of the *Fgpal1*/*FgPAL1*-GFP transformant were treated with Lat-A for 10 min and examined by epifluorescence microscopy. Bar = 20 μm. D. Hyphae of the *Fgpal1*/LifeAct-RFP and PH-1/LifeAct-RFP transformant were examined by epifluorescence microscopy. Bar = 20 μm. [Color figure can be viewed at wileyonlinelibrary.com]

we generated the *FgEDE1*-GFP construct and transformed it into the *Fgpal1* mutant and PH-1. In the wild type background, FgEde1-GFP signals localized to the sub-apical regions at hyphal tips (Fig. 5B), which was similar to the localization of FgPal1-GFP. In the *Fgpal1*/*FgEDE1*-GFP transformant, however, the enrichment of FgEde1-GFP signals in the sub-apical region was not observed although faint, diffused FgEde1-GFP signals were observed in the rear region of hyphal tips (Fig. 5B). These results suggested that FgPal1 may play a role in the localization of FgEde1 via the CME.

FgPal1 localizes to the septum during cytokinesis

Fungal cytokinesis requires the formation of the septum cell wall, which is tightly coordinated with the contraction of cytokinetic actomyosin ring (CAR) (Berepiki *et al*., 2011). In *F. graminearum*, FgPal1 is also localized to the septum. In the transformants expressing both LifeAct-RFP and *FgPAL1*-GFP constructs, partial co-localization of LifeAct and FgPal1 was observed (Fig. 6A). However, in comparison with LifeAct-RFP signals, FgPal1-GFP signals were relatively weak at septa (Fig. 6A).

To characterize the role of FgPal1 in septation, we analysed the spatio-temporal association of FgPal1-GFP and LifeAct-RFP during septum formation. LifeAct-RFP signals representing F-actin cables became visible as the septal actin tangle (SAT) at the septation site (Seiler and Heilig, 2019) (Fig. 6B). However, weak GFP signals were observed only after the contraction of the actin ring and the formation of septa (Fig. 6B). These results suggest that localization of FgPal1-GFP to the septum only occurred at late stages of septum formation. Therefore, FgPal1 is not important for the localization of SAT and

constriction of CAR in *F. graminearum*, which is different from its orthologue in *S. cerevisiae* (Ge *et al*., 2005; Carroll *et al*., 2012).

To further determine the role of F-actin in the maintenance of FgPal1 at the division site, the *Fgpal1*/*FgPAL1*-GFP transformant were treated with Lat-A and DMSO as a control for10 min. In LatA-treated hyphae, FgPal1-GFP signals were still observed at septa (Fig. 6C), indicating that localization of FgPal1 to the septum is independent of F-actin (Fig. 6C). In the *Fgpal1* LifeAct-GFP transformant, the localization of LifeAct-GFP at the septum also was not affected by deletion of *FgPAL1* (Fig. 6D). These results indicated that the assembly of F-actin at the septum was independent of FgPal1. Thus, the localization of FgPal1 and LifeAct to the septum is not interdependent, which is different from their dynamic association at the sub-apical collar of hyphal tips.

The localization of FgPal1 in hyphae is independent of FgKin1 and FgPom1 kinases

In the fission yeast, protein kinases Kin1 and Pom1 phosphorylate Pal1 at distinct sites to promote its localization to the tip region of the growing end (Koyano *et al*., 2010; Lee *et al*., 2018). The *Fgkin1* and *Fgpom1* mutants generated in previous studies have defects in hyphal growth, pathogenesis and sexual reproduction in *F. graminearum* (Wang *et al*., 2011; Luo *et al*., 2014). We also transformed the *FgPAL1*-GFP construct into the *Fgkin1* and *Fgpom1* mutants. In the resulting transformants, FgPal1-GFP still localized to the collar region at hyphal tips (Fig. S3A). Localization of FgPal1-GFP to the septum also was observed in the *Fgkin1* and *Fgpom1* mutants (Fig. S3B). These results indicate that the localization of FgPal1 to the hyphal tip collar or septum is not affected by deletion of *FgKIN1* or *FgPOM1* in *F. graminearum*. Therefore, whether FgPal1 is phosphorylated by FgKin1 and FgPom1 or not, its localization is independent of these two protein kinases.

Deletion of FgPAL1 *affects the distribution of nuclei in conidia and vegetative hyphae*

To determine whether deletion of *FgPAL1* affects cytokinesis and nuclear distribution, we transformed an H1-GFP fusion construct (Chen *et al*., 2018) into PH-1 and the *Fgpal1* mutant M8. When the resulting transformants were examined by epifluorescence microscopy, most of the wild-type conidia (76.3 ± 25.4%) had one nucleus in each compartment (Fig. 7A). However, the majority (52.5 ± 24.3%) of the *Fgpal1* mutant conidia had two or more nuclei per compartment. Similarly, the *Fgpal1* mutant had more nuclei (3.2 ± 0.1) per compartment than the wild type in vegetative hyphae (2.5 ± 0.2)

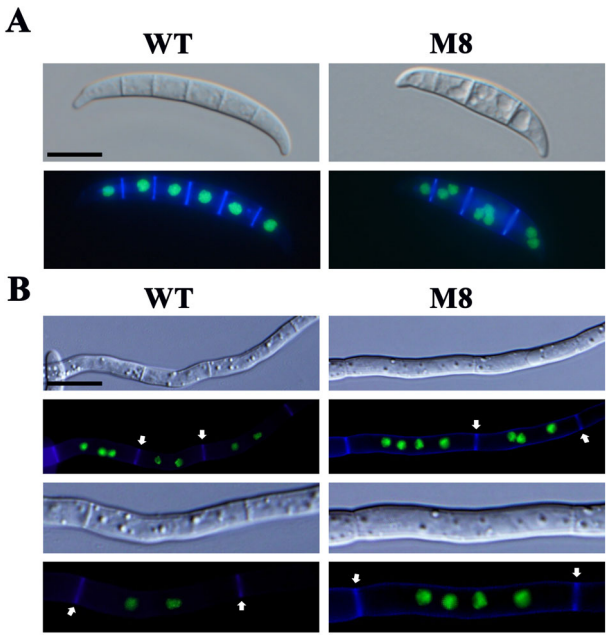

Fig. 7. Defects of the *Fgpal1* mutant in the distribution of nuclei and septa. (A) Conidia and (B) vegetative hyphae of transformants of PH-1 and the *Fgpal1* mutant (M8) expressing the H1-GFP construct were stained with Calcofluor white (CFW) and examined by DIC and epifluorescence microscopy. Arrows point to the septum. Bar = 20 μm. [Color figure can be viewed at wileyonlinelibrary.com]

(Fig. 7B). Calcofluor white (CFW) staining showed that the *Fgpal1* mutant still formed septa in conidia (Fig. 7A) and vegetative hyphae (Fig. 7B) but mutant conidia had fewer septa and mutant hyphae had irregular distance between septa. These results indicated that the *Fgpal1* mutant may be defective in the coordination between nuclear division and cytokinesis or suppression of nuclear division after septation during asexual reproduction or vegetative growth.

FgPAL1 *is dispensable for meiosis but important for ascospore formation*

We then examined nuclear behaviours during ascus and ascospore development in perithecia formed by the *Fgpal1* H1-GFP transformant. At 5 dpf, the wild type developed asci with eight nuclei but only croziers with two nuclei or developing asci with one nucleus were observed in the *Fgpal1* H1-GFP transformant (Fig. 8A). Nevertheless, many developing asci with eight nuclei were observed in the *Fgpal1* mutant at 7 dpf (Fig. 8A), indicating that meiosis was delayed, likely due to the reduced growth rate associated with deletion of *FgPAL1* in *F. graminearum*.

As described above, majority of *Fgpal1* asci were aborted and lacked ascospores. When examined by epifluorescence microscopy, no nuclei were observed in the

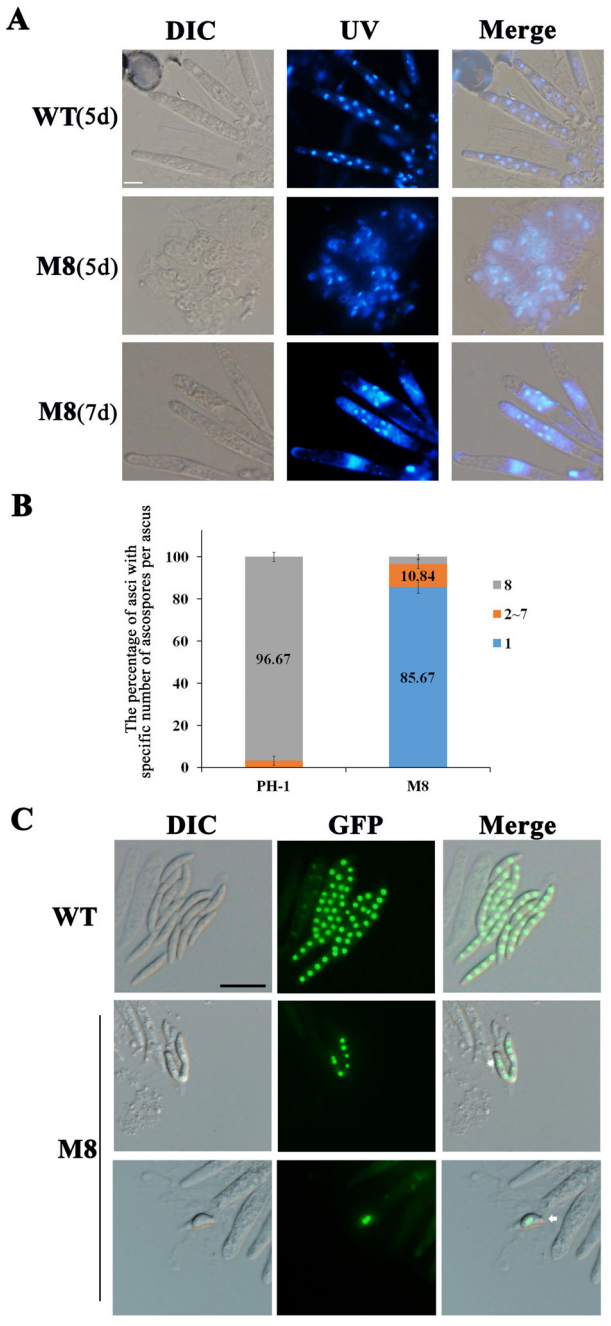

Fig. 8. Defects of the *Fgpal1* mutant in the distribution of nuclei during sexual reproduction. A. Perithecia formed by H1-GFP transformants of PH-1 and the *Fgpal1* mutant were examined for ascogenous tissues at 5 or 7 dpf. Bar = 20 μm. B. The percentage of wild-type or *Fgpal1* asci with the indicated number of ascospores per ascus in perithecia at 12-dpf. The vast majority of *Fgpal1* asci had only one ascospore. C. Asci and ascospores formed by H1-GFP transformants of PH-1 and the *Fgpal1* mutant were examined for GFP signals at 12-dpf. [Color figure can be viewed at wileyonlinelibrary.com]

aborted asci with granular cytoplasm at 12 dpf. For the few ascospores formed by the *Fgpal1* mutant, they varied significantly in morphology and the number of nuclei in each ascospore (Fig. 8B and C). Most of the *Fgpal1* ascospores had less than four nuclei and fewer than four compartments. These results indicate that *FgPAL1* plays an important role in nuclear distribution in developing asci during ascospore formation. Ascospore formation was defective in the *Fgpal1* mutant, probably because of the important role played by *FgPAL1* during ascospore delimitation (cell wall formation during the free cell formation process) and the coordination between cytokinesis and post-meiotic mitosis in developing asci.

Both FtsK and PAL1 domains are essential for the function of FgPal1

To determine the function of the FtsK and PAL1 domains, we generated the *FgPAL1*$^{\Delta FtsK}$ and *FgPAL1*$^{\Delta PAL1}$ constructs and transformed them into the *Fgpal1* mutant M8. The resulting *FgPAL1*$^{\Delta FtsK}$ and *FgPAL1*$^{\Delta PAL1}$ transformants (Table 1), similar to the original *Fgpal1* mutant, were reduced in growth rate (Fig. 9A). They also were defective in ascospore releasing (Fig. 9B) and had defects in ascospore budding inside asci (Fig. 9C). These results indicated that both FtsK and PAL1 domains are essential for the function of FgPal1 in *F. graminearum*.

Discussion

In both budding and fission yeasts, Pal1 is related to endocytosis and cell polarity although its exact function is not clear. The Pal1 orthologues with a characteristic PAL1 domain are well conserved in fungi. To date, no proteins with the PAL11 domain have been identified in plants and metazoans. Because the PAL1 domain is unique to fungi, FgPal1 orthologues likely have fungal-specific biological functions. Furthermore, the FgPal1 protein and its orthologues from other filamentous ascomycetes also contain an FtsK domain towards the N-terminal region. The FtsK domain has a putative ATP binding P-loop motif. It is first identified in the cell division gene *ftsK* of *Escherichia coli* and assumed to be involved in DNA movement coupling with ATP hydrolysis in bacteria (Steiner *et al*., 1999; Stouf *et al*., 2013). In eukaryotic organisms, no proteins with the FtsK domain have been functionally characterized. In this study, we showed that both FtsK and PAL1 domains are essential for the functions of FgPal1 in *F. graminearum*. With both a fungal-specific PAL1 domain and a bacterial FtsK domain, FgPal1 may play a unique role in regulating hyphal growth, nuclear distribution and differentiation in filamentous fungi.

In *F. graminearum*, the *Fgpal1* deletion mutant was defective in maintaining polarized growth at the tip and often had apical or subapical swollen bodies. In *S. cerevisiae*, the *pal1* mutant forms pearl- and lemon-

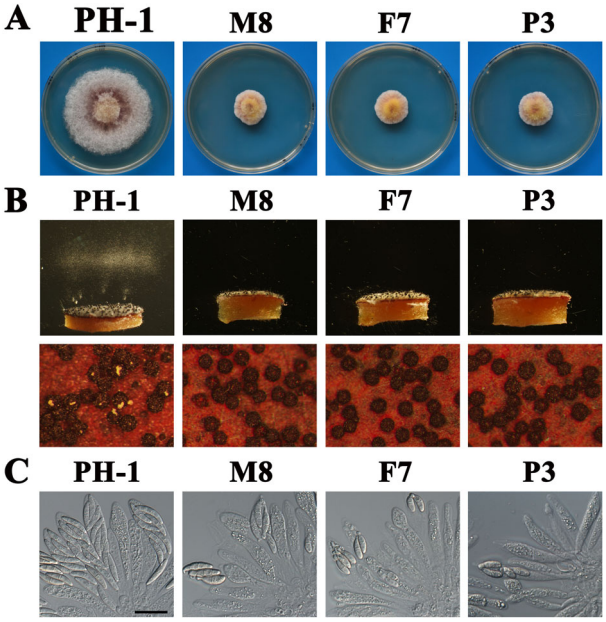

Fig. 9. Defects of the *FgPAL1*$^{\Delta PAL1}$ and *FgPAL1*$^{\Delta FtsK}$ mutants in vegetative growth, conidium morphology and sexual reproduction. A. Three-day-old PDA cultures of the wild-type (PH-1), *Fgpal1* (M8), *FgPAL1*$^{\Delta PAL1}$ (F7) and *FgPAL1*$^{\Delta FtsK}$ (P3) mutant strains. B. Perithecia of the same set of strains were assayed for ascospore discharge (upper row) and cirrhus formation (lower row). D. Asci and ascospores formed by the marked strains. Similar to the *Fgal1* mutant, the *FgPAL1*$^{\Delta PAL1}$ and *FgPAL1*$^{\Delta FtsK}$ mutants had ascospore budding defects. Bar = 20 μm. [Color figure can be viewed at wileyonlinelibrary.com]

shaped yeast cells (Ge *et al*., 2005). Deletion of its orthologue in *S. pombe* also resulted in the formation of yeast cells with abnormal morphology (Ge *et al*., 2005). Nevertheless, the *pal1* mutants still produce some normal yeast cells in both *S. cerevisiae* and *S. pombe*. Similarly, the *Fgpal1* mutant still produces cylindrical hyphae although many of them have deformed hyphal tips. Therefore, the Pal1 orthologues may have a conserved but non-essential function in the maintenance of cell shape and polarity in filamentous fungi. Nevertheless, besides the defect in hyphal tip morphology, the *Fgpal1* mutant was significantly reduced in growth rate, which is different from the *pal1* mutants in *S. pombe* (Kettenbach *et al*., 2015). Previous studies have shown that endocytosis is related to hyphal growth in other fungi (Penalva, 2010; Steinberg, 2014). The *Fgpal1* mutant was not only defective in general endocytosis as assayed by the uptake of the lipophilic dye FM4-64 but also defective in the sub-apical localization of endocytic scaffolding protein FgEde1.

In actively growing hyphae of *F. graminearum*, FgPal1-GFP is mainly localized to the collar region of hyphal tips. Treatments with Lat-A, an F-actin inhibitor that depolymerizes actin filaments, resulted in the re-localization of FgPal1-GFP to hyphal tips, suggesting that the localization of FgPal1 to the subapical collar depends on F-actins. In *S. pombe*, the localization of Pal1 to the growing end and division site is independent of F-actin (Ge *et al*., 2005). F-actin is required to capture the secretory vesicles and transported them to the site of exocytosis and endocytosis for tip expansion (Brand and Gow, 2009). In transformants expressing both LifeAct-RFP and FgPal1-GFP, partial colocalization of LifeAct and FgPal1 was observed in the collar region. However, only LifeAct was observed in the very apex of hyphal tips that overlaps with the polarisome, which supports actin-filament elongation (Guo *et al*., 2015). Deletion of *FgPAL1* affected the apex localization of LifeAct in the *Fgpal1* LifeAct-GFP transformant. Thus, FgPal1 may affect the actin cable dynamics and transportation of vesicles to the hyphal tip in *F. graminearum*.

Ede1 is one of the early phase proteins in CME that arrive at the endocytic site and plays a key role in endocytic site initiation and maturation (Brach *et al*., 2014; Han *et al*., 2020). In our study, deletion of *FgPAL1* affected the sub-apical localization of endocytic scaffolding protein FgEde1. The *Fgpal1* mutant was defective in general endocytosis of FM4-64. Thus, FgPal1 may affect the transportation of vesicles to the hyphal tip by both general endocytosis and CME. However, *FgPAL1* is not essential for polarity establishment or maintenance because the localization of FgSpa2 to hyphal tips was not affected in the *Fgpal1* mutant. Recently, components of the FgAP-2 complex that functions as a cargo-specific adaptor for endocytosis have been reported to localize to the subapical collar in *F. graminearum* (Zhang *et al*., 2019). Therefore, it is important to determine the co-localization and possible functional relationship between FgPal1 and the FgAP-2 complex in endocytosis at the collar region of hyphal tips.

In eukaryotic cells, cytokinesis is the final step in the cell cycle that is regulated by septation initiation network (SIN), which triggers the contraction of the actomyosin ring and formation of the division septum. Deficiencies in SIN signalling result in cytokinesis failures and the formation of multinucleated cells (Simanis, 2015). In *F. graminearum*, the *Fgpal1* mutants were defective in the distribution of nuclei in hyphae and tended to have more nuclei per compartment than the wild type. In comparison with normal conidia with one nucleus per compartment, *Fgpal1* conidia had fewer compartments or septa but most of the compartments had more than one nucleus, likely due to its defects in septation. Therefore, *FgPAL1* likely plays a role in normal cytokinesis during growth and asexual reproduction. However, septation and formation of F-actin rings were still observed in the *Fgpal1* mutant. Furthermore, FgPal1-GFP signals only became visible at the septation site in hyphae after the constriction of the actin ring and septum formation, which

is different from the presence of Pal1 at the division site before actin being assembled in *S. cerevisiae* and *S. pombe* (Ge *et al*., 2005; Kettenbach *et al*., 2015).

During sexual reproduction, the *Fgpal1* mutant was able to form asci with eight nuclei, indicating that FgPal1 is not essential for meiosis and the post-meiotic mitosis before the delimitation of ascospores. However, most of the developing asci became aborted and only a few of them formed ascospores in the *Fgpal1* mutant, suggesting the importance of *FgPAL1* in ascospore formation or delimitation. The defect of *Fgpal1* in forming fewer than eight ascospores per ascus may be also related to its functions in the nuclear distribution and cytokinesis in developing asci. Although components of the FgAP-2 complex had similar localization with FgPal1, their mutants were normal in ascospore development (Zhang *et al*., 2019), suggesting that FgPal1 and the FgAP-2 complex differ significantly in functions during sexual reproduction. After meiosis, the formation of ascospore wall for each haploid nucleus or the delimitation of ascospores inside asci involves the free cell formation process that has not been well characterized at the molecular level in filamentous ascomycetes. FgPal1 and its orthologues may play an important role in the free cell formation process for ascospore formation.

Materials and methods

Strains and culture conditions

The wild-type strain PH-1 (Cuomo *et al*., 2007) and mutant strains of *F. graminearum* generated in this study were routinely cultured on CM, SYM (1% starch, 0.6% yeast extract, 0.3% sucrose and 2% agar) (Yang *et al*., 2017), and 5× YEG plates at 25°C. The growth rate on CM and 5× YEG plates, conidiation in liquid CMC cultures and mating on carrot agar plates were assayed as previously described (Hou *et al*., 2002; Zhou *et al*., 2010; Cavinder *et al*., 2012; Cao *et al*., 2016). Protoplast preparation and polyethylene glycol-mediated transformation were performed as described (Wang *et al*., 2011). Hygromycin B (CalBiochem, La Jolla, CA, USA) and geneticin (Sigma-Aldrich, St Louis, MO, USA) were added to the final concentration of 300 and 400 μg ml^{-1} respectively, for transformant selection (Wang *et al*., 2011). DON production in infected wheat kernels was assayed as described previously (Jiang *et al*., 2016). Conidia harvested from 5 day-old CMC cultures were used to measure the length and number of septation or nuclei in each compartment as described (Chen *et al*., 2014). The number of nuclei per hyphal compartment and branching distance were measured with hyphae from 24 yeast extract peptone dextrosemedium cultures (Li *et al*., 2015). Mean and standard deviation were calculated with data from three independent replicates, with at least 100 conidia, 100 hyphal branches, or 50 hyphal compartments examined per replicate.

Generation of the Fgpal1 *deletion mutant and complemented transformant*

The same primers used in the previous study (Hao *et al*., 2019) were used to generate additional *Fgpal1* gene replacement mutants with the split-marker approach. For complementation assays, the *FgPAL1* gene with its full-length promoter region was amplified with primer pairs *FgPAL1*NC/1F-*FgPAL1*NC/2R and co-transformed with *Xho*I-digested pDL2 into yeast strain XK1-25 to generate the *FgPAL1*-GFP construct by yeast gap repair as described (Bruno *et al*., 2004; Zhou *et al*., 2010). After verification by sequencing analysis, the *FgPAL1*-GFP construct was transformed into the *Fgpal1*, *Fgkin1* (Luo *et al*., 2014) and *Fgpom1* (Wang *et al*., 2011) mutants. Transformants expressing the *FgPAL1*-GFP construct were identified by PCR and examined for GFP signals by epifluorescence microscopy. The same yeast gap repair approach (Bruno *et al*., 2004; Zhou *et al*., 2010) was used to generate the $FgPAL1^{\Delta FtsK}$ and $FgPAL1^{\Delta PAL1}$ alleles deleted of the FtsK and PAL1 domains with primers listed in Table S1. The resulting $FgPAL1^{\Delta PAL1}$ and $FgPAL1^{\Delta FtsK}$ alleles were verified by sequencing analysis and transformed into the *Fgpal1* mutant M8.

The H1-GFP construct (Luo *et al*., 2014) was transformed into the wild-type strain PH-1 and the *Fgpal1* mutant to observe nuclei. The FgSpa2-GFP construct was generated by yeast gap repair as described (Bruno *et al*., 2004; Zhou *et al*., 2010) and transformed into the wild-type strain PH-1 and the *Fgpal1* mutant to observe the polarisome (Zhang *et al*., 2019). Cell wall and septa were visualized by staining conidia or hyphae with 10 μg/ml^{-1} CFW for 2 min and observed with an Olympus BX-53 microscope as described (Luo *et al*., 2014; Li *et al*., 2015)

Generation of the LifeAct-RFP FgPAL1-*GFP transformant*

The LifeAct fragment consisting of the first 17 aa residues of yeast actin-binding protein Abp140 is an F-actin marker in eukaryotes (Lopata *et al*., 2018). The LifeAct-RFP construct (Zhang *et al*., 2019) was co-transformed with *FgPAL1*-GFP into the wild-type strain PH-1. Transformants resistant to geneticin were isolated and screened by PCR. Transformants expressing both LifeAct-RFP and *FgPAL1*-GFP were further confirmed by examination for RFP and GFP signals. The co-localization of LifeAct-RFP and FgPal1-GFP was

observed with a Nikon A1 confocal microscope. The excitation and emission wavelengths for GFP were 488 and 500–550 nm. For RFP, the excitation and emission wavelengths were 561 and 570–620 nm (Petre *et al*., 2015; Boenisch *et al*., 2019). For assaying the role of actin on the localization of FgPal1-GFP, vegetative hyphae harvested from SYM cultures were treated with 0.1 μg ml^{-1} Lat-A (Sigma-Aldrich, St. Louis, MO) in DMSO for 10–30 min (Ge *et al*., 2005) before examination by epifluorescence microscopy.

Assays for virulence and infectious growth

Conidia were harvested from 5-day-old CMC cultures and re-suspended to 2.0×10^5 conidia per ml in sterile distilled water (Hou *et al*., 2002). Wheat heads of cultivar Xiaoyan 22 were drop-inoculated and examined for FHB symptoms as described (Zhang *et al*., 2017). Spikelets with typical head blight symptoms in each head were examined at 14 dpi to estimate the disease index (Ding *et al*., 2009). Infection assays with corn silks were conducted as described (Hou *et al*., 2002). All the infection assays were repeated at least three times.

For assaying infectious growth, wheat lemmas and rachis tissues were collected from inoculated wheat heads and fixed with 4% (vol./vol.) glutaraldehyde in 0.1 M phosphate buffer (pH 6.8) overnight at 4°C, dehydrated and embedded in Spurr resin as described (Kang *et al*., 2008). Thick sections (1 μm) were stained with 0.5% (wt./vol.) toluidine blue and examined with an Olympus BX-53 microscope as described (Zheng *et al*., 2012). At least three independent biologic replicates were examined for the wild-type and mutant strains.

Yeast two-hybrid assays

The HybriZAP bait and prey system (Delgado-Álvarez *et al*., 2010; Zhou *et al*., 2012) was used to detect the interaction of FgPal1 with FgAma1. In brief, the bait construct of *FgPAL1* was generated by cloning the full-length *FgPAL1* ORF with primers Pal1AD/F and Pal1AD/R (Table S1) into pAD-GAL4. The full-length FgAma1 was amplified with primers Ama1BD/F and Ama1BD/R (Table S1) and cloned into pBD-GAL4-2 as the prey construct. The resulting bait and prey constructs were co-transformed into the yeast strain YRG2 as described (Delgado-Álvarez *et al*., 2010; Zhou *et al*., 2012). The resulting Leu+ and Trp+ transformants were assayed for growth on SD-Trp-Leu-His medium and the expression of the LacZ reporter as described (Li *et al*., 2017).

Acknowledgements

We thank Dr. Cong Jiang and Dr. Huiquan Liu for fruitful discussion and Dr. Larry Dunkle for critical reading of this manuscript. We also thank Dr. Hua Zhao (State Key Laboratory of Crop Stress Biology for Arid Areas, Northwest A&F University, Yangling, China) for microscope experimental assistance. This work was supported by a grant to Guanghui Wang from the National Natural Science Foundation of China (No. 31801684), a grant to Ping Xiang from the Key Research and Invention Program in Shaanxi Province of China (2018NY-107), and a grant to J.-R.X. from USWBSI.

References

Araujo-Bazán, L., Peñalva, M.A., and Espeso, E.A. (2008) Preferential localization of the endocytic internalization machinery to hyphal tips underlies polarization of the actin cytoskeleton in *Aspergillus nidulans*. *Mol Microbiol* **67**: 891–905.

Bai, G.H., and Shaner, G. (2004) Management and resistance in wheat and barley to Fusarium head blight. *Annu Rev Phytopathol* **42**: 135–161.

Berepiki, A., Lichius, A., and Read, N.D. (2011) Actin organization and dynamics in filamentous fungi. *Nat Rev Microbiol* **9**: 876–887.

Bian, Z., Ni, Y., Xu, J.-R., and Liu, H. (2019) A-to-I mRNA editing in fungi: occurrence, function, and evolution. *Cell Mol Life Sci* **76**: 329–340.

Boenisch, M.J., Blum, A., Broz, K.L., Gardiner, D.M., and Kistler, H.C. (2019) Nanoscale enrichment of the cytosolic enzyme trichodiene synthase near reorganized endoplasmic reticulum in *Fusarium graminearum*. *Fungal Genet Biol* **124**: 73–77.

Boenisch, M.J., and Schäfer, W. (2011) *Fusarium graminearum* forms mycotoxin producing infection structures on wheat. *BMC Plant Biol* **11**: 110–110.

Brach, T., Godlee, C., Moeller-Hansen, I., Boeke, D., and Kaksonen, M. (2014) The initiation of clathrin-mediated endocytosis is mechanistically highly flexible. *Curr Biol* **24**: 548–554.

Brand, A., and Gow, N.A.R. (2009) Mechanisms of hypha orientation of fungi. *Curr Opin Microbiol* **12**: 350–357.

Bruno, K.S., Tenjo, F., Li, L., Hamer, J.E., and Xu, J.R. (2004) Cellular localization and role of kinase activity of PMK1 in *Magnaporthe grisea*. *Eukaryot Cell* **3**: 1525–1532.

Cao, S., He, Y., Hao, C., Xu, Y., Zhang, H., Wang, C., *et al*. (2017) RNA editing of the *AMD1* gene is important for ascus maturation and ascospore discharge in *Fusarium graminearum*. *Sci Rep* **7**: 4617.

Cao, S.L., Zhang, S.J., Hao, C.F., Liu, H.Q., Xu, J.R., and Jin, Q.J. (2016) FgSsn3 kinase, a component of the mediator complex, is important for sexual reproduction and pathogenesis in *Fusarium graminearum*. *Sci Rep* **6**: 22333.

Carroll, S.Y., Stimpson, H.E., Weinberg, J., Toret, C.P., Sun, Y., and Drubin, D.G. (2012) Analysis of yeast endocytic site formation and maturation through a regulatory transition point. *Mol Biol Cell* **23**: 657–668.

Cavinder, B., Sikhakolli, U., Fellows, K.M., and Trail, F. (2012) Sexual development and ascospore discharge in *Fusarium graminearum*. *Jove-J Vis Exp*, **61**. https://doi.org/10.3791/3895.

Chen, D., Wang, Y., Zhou, X., Wang, Y., and Xu, J.-R. (2014) The Sch9 kinase regulates conidium size, stress responses, and pathogenesis in *Fusarium graminearum*. *PLoS One* **9**: e105811.

Chen, D., Wu, C., Hao, C., Huang, P., Liu, H., Bian, Z., *et al*. (2018) Sexual specific functions of Tub1 beta-tubulins require stage-specific RNA processing and expression in *Fusarium graminearum*. *Environ Microbiol* **20**: 4009–4021.

Cooper, K.F., Mallory, M.J., Egeland, D.B., Jarnik, M., and Strich, R. (2000) Ama1p is a meiosis-specific regulator of the anaphase promoting complex/cyclosome in yeast. *Proc Natl Acad Sci U S A* **97**: 14548–14553.

Cuomo, C.A., Gueldener, U., Xu, J.R., Trail, F., Turgeon, B. G., Di Pietro, A., *et al*. (2007) The *Fusarium graminearum* genome reveals a link between localized polymorphism and pathogen specialization. *Science* **317**: 1400–1402.

Delgado-Álvarez, D.L., Callejas-Negrete, O.A., Gómez, N., Freitag, M., Roberson, R.W., Smith, L.G., *et al*. (2010) Visualization of F-actin localization and dynamics with live cell markers in *Neurospora crassa*. *Fungal Genet Biol* **47**: 573–586.

Ding, S.L., Mehrabi, R., Koten, C., Kang, Z.S., Wei, Y.D., Seong, K.Y., *et al*. (2009) Transducin Beta-like gene *FTL1* is essential for pathogenesis in *Fusarium graminearum*. *Eukaryot Cell* **8**: 867–876.

Fischer-Parton, S., Parton, R.M., Hickey, P.C., Dijksterhuis, J., Atkinson, H.A., and Read, N.D. (2000) Confocal microscopy of FM4-64 as a tool for analysing endocytosis and vesicle trafficking in living fungal hyphae. *J Microsc* **198**: 246–259.

Ge, W.Z., Chew, T.G., Wachtler, V., Naqvi, S.N., and Balasubramanian, M.K. (2005) The novel fission yeast protein Pal1p interacts with Hip1-related Sla2p/End4p and is involved in cellular morphogenesis. *Mol Biol Cell* **16**: 4124–4138.

Goswami, R.S., and Kistler, H.C. (2004) Heading for disaster: *Fusarium graminearum* on cereal crops. *Mol Plant Pathol* **5**: 515–525.

Guo, M., Kilaru, S., Schuster, M., Latz, M., and Steinberg, G. (2015) Fluorescent markers for the Spitzenkörper and exocytosis in *Zymoseptoria tritici*. *Fungal Genet Biol* **79**: 158–165.

Han, X., Chen, L., Li, W., Zhang, L., Zhang, L., Zou, S., *et al*. (2020) Endocytic FgEde1 regulates virulence and autophagy in *Fusarium graminearum*. *Fungal Genet Biol* **141**: 103400.

Hane, J.K., Williams, A.H., Taranto, A.P., Solomon, P.S., and Oliver, R.P. (2015) Repeat-induced point mutation: a fungal-specific, endogenous mutagenesis process. In *Genetic Transformation Systems in Fungi*, Vol. **2**, van den Berg, M.A., and Maruthachalam, K. (eds). Cham: Springer International Publishing, pp. 55–68.

Hao, C., Yin, J., Sun, M., Wang, Q., Liang, J., Bian, Z., *et al*. (2019) The meiosis-specific APC activator *FgAMA1* is dispensable for meiosis but important for ascosporogenesis in *Fusarium graminearum*. *Mol Microbiol* **111**: 1245–1262.

Hou, Z.M., Xue, C.Y., Peng, Y.L., Katan, T., Kistler, H.C., and Xu, J.R. (2002) A mitogen-activated protein kinase gene (*MGV1*) in *Fusarium graminearum* is required for female fertility, heterokaryon formation, and plant infection. *Mol Plant Microbe Interact* **15**: 1119–1127.

Jiang, C., Cao, S., Wang, Z., Xu, H., Liang, J., Liu, H., *et al*. (2019) An expanded subfamily of G-protein-coupled receptor genes in *Fusarium graminearum* required for wheat infection. *Nat Microbiol* **4**: 1582–1591.

Jiang, C., Zhang, C., Wu, C., Sun, P., Hou, R., Liu, H., *et al*. (2016) *TRI6* and *TRI10* play different roles in the regulation of deoxynivalenol (DON) production by cAMP signalling in *Fusarium graminearum*. *Environ Microbiol* **18**: 3689–3701.

Kang, Z.S., Buchenauer, H., Huang, L.L., Han, Q.M., and Zhang, H.C. (2008) Cytological and immunocytochemical studies on responses of wheat spikes of the resistant Chinese cv. Sumai 3 and the susceptible cv. Xiaoyan 22 to infection by *Fusarium graminearum*. *Eur J Plant Pathol* **120**: 383–396.

Kettenbach, A.N., Deng, L., Wu, Y.J., Baldissard, S., Adamo, M.E., Gerber, S.A., *et al*. (2015) Quantitative phosphoproteomics reveals pathways for coordination of cell growth and division by the conserved fission yeast kinase Pom1. *Mol Cell Proteomics* **14**: 1275–1287.

Kim, H.-K., Jo, S.-M., Kim, G.-Y., Kim, D.-W., Kim, Y.-K., and Yun, S.-H. (2015) A large-scale functional analysis of putative target genes of mating-type loci provides insight into the regulation of sexual development of the cereal pathogen *Fusarium graminearum*. *PLoS Genet* **11**: e1005486.

Koyano, T., Kume, K., Konishi, M., Toda, T., and Hirata, D. (2010) Search for kinases related to transition of growth polarity in fission yeast. *Biosci Biotechnol Biochem* **74**: 1129–1133.

Lee, M.E., Rusin, S.F., Jenkins, N., Kettenbach, A.N., and Moseley, J.B. (2018) Mechanisms connecting the conserved protein kinases Ssp1, Kin1, and Pom1 in fission yeast cell polarity and division. *Curr Biol* **28**: 84–92.

Li, C., Melesse, M., Zhang, S., Hao, C., Wang, C., Zhang, H., *et al*. (2015) *FgCDC14* regulates cytokinesis, morphogenesis and pathogenesis in *Fusarium graminearum*. *Mol. Microbiol.* **98**: 770–786.

Li, G., Zhang, X., Tian, H., Choi, Y.E., Tao, W.A., and Xu, J. R. (2017) *MST50* is involved in multiple MAP kinase signaling pathways in *Magnaporthe oryzae*. *Environ Microbiol* **19**: 1959–1974.

Liu, H., Wang, Q., He, Y., Chen, L., Hao, C., Jiang, C., *et al*. (2016) Genome-wide A-to-I RNA editing in fungi independent of ADAR enzymes. *Genome Res* **26**: 499–509.

Lopata, A., Hughes, R., Tiede, C., Heissler, S.M., Sellers, J. R., Knight, P.J., *et al*. (2018) Affimer proteins for F-Actin: novel affinity reagents that label F-Actin in live and fixed cells. *Sci Rep* **8**: 6572.

Lu, R., and Drubin, D.G. (2017) Selection and stabilization of endocytic sites by Ede1, a yeast functional homologue of human Eps15. *Mol Biol Cell* **28**: 567–575.

Luo, Y.P., Zhang, H.C., Qi, L.L., Zhang, S.J., Zhou, X.Y., Zhang, Y.M., *et al*. (2014) FgKin1 kinase localizes to the septal pore and plays a role in hyphal growth, ascospore germination, pathogenesis, and localization of Tub1 beta-

tubulins in *Fusarium graminearum*. *New Phytol* **204**: 943–954.
Markell, S.G., and Francl, L.J. (2003) Fusarium head blight inoculum: species prevalence and *Gibberella zeae* spore type. *Plant Dis* **87**: 814–820.
Miedaner, T., Cumagun, C.J.R., and Chakraborty, S. (2008) Population genetics of three important head blight pathogens *Fusarium graminearum*, *F. pseudograminearum* and *F. culmorum*. *J Phytopathol* **156**: 129–139.
Nakayashiki, H. (2005) RNA silencing in fungi: mechanisms and applications. *FEBS Lett* **579**: 5950–5957.
Penalva, M.A. (2010) Endocytosis in filamentous fungi: Cinderella gets her reward. *Curr Opin Microbiol* **13**: 684–692.
Petre, B., Saunders, D.G.O., Sklenar, J., Lorrain, C., Win, J., Duplessis, S., *et al*. (2015) Candidate effector proteins of the rust pathogen *Melampsora larici-populina* target diverse plant cell compartments. *Mol Plant Microbe Interact* **28**: 689–700.
Seiler, S., and Heilig, Y. (2019) Septum formation and cytokinesis in ascomycete fungi. In *Biology of the Fungal Cell*, Hoffmeister, D., and Gressler, M. (eds). Cham: Springer International Publishing, pp. 15–42.
Simanis, V. (2015) Pombe's thirteen - control of fission yeast cell division by the septation initiation network. *J Cell Sci* **128**: 1465–1474.
Son, H., Min, K., Lee, J., Raju, N.B., and Lee, Y.-W. (2011) Meiotic silencing in the homothallic fungus *Gibberella zeae*. *Fungal Biol* **115**: 1290–1302.
Steinberg, G. (2014) Endocytosis and early endosome motility in filamentous fungi. *Curr Opin Microbiol* **20**: 10–18.
Steiner, W., Liu, G., Donachie, W.D., and Kuempel, P. (1999) The cytoplasmic domain of FtsK protein is required for resolution of chromosome dimers. *Mol Microbiol* **31**: 579–583.
Stouf, M., Meile, J.-C., and Cornet, F. (2013) FtsK actively segregates sister chromosomes in *Escherichia coli*. *Proc Natl Acad Sci U S A* **110**: 11157–11162.
Takeshita, N., and Fischer, R. (2019) The cytoskeleton and polarity markers during polarized growth of filamentous fungi. In *Biology of the Fungal Cell*, Hoffmeister, D., and Gressler, M. (eds). Cham: Springer International Publishing, pp. 43–62.
Teichert, I., Dahlmann, T.A., Kück, U., and Nowrousian, M. (2017) RNA editing during sexual development occurs in distantly related filamentous ascomycetes. *Genome Biol Evol* **9**: 855–868.
Trail, F., Xu, H.X., Loranger, R., and Gadoury, D. (2002) Physiological and environmental aspects of ascospore discharge in *Gibberella zeae* (anamorph *Fusarium graminearum*). *Mycologia* **94**: 181–189.
Van de Walle, J., Sergent, T., Piront, N., Toussaint, O., Schneider, Y.J., and Larondelle, Y. (2010) Deoxynivalenol affects *in vitro* intestinal epithelial cell barrier integrity through inhibition of protein synthesis. *Toxicol Appl Pharmacol* **245**: 291–298.
Wang, C.F., Zhang, S.J., Hou, R., Zhao, Z.T., Zheng, Q., Xu, Q.J., *et al*. (2011) Functional analysis of the kinome of the wheat scab fungus *Fusarium graminearum*. *PLoS Pathog* **7**: e1002460.
Yang, C.D., Dang, X., Zheng, H.W., Chen, X.F., Lin, X.L., Zhang, D.M., *et al*. (2017) Two Rab5 homologs are essential for the development and pathogenicity of the rice blast fungus *Magnaporthe oryzae*. *Front Plant Sci* **8**: 620.
Zhang, H., Van der Lee, T., Waalwijk, C., Chen, W.Q., Xu, J., Xu, J.S., *et al*. (2012) Population analysis of the *Fusarium graminearum* species complex from wheat in China show a shift to more aggressive isolates. *PLoS One* **7**: e31722.
Zhang, J., Yun, Y., Lou, Y., Abubakar, Y.S., Guo, P., Wang, S., *et al*. (2019) FgAP-2 complex is essential for pathogenicity and polarised growth and regulates the apical localisation of membrane lipid flippases in *Fusarium graminearum*. *Cell Microbiol* **21**: e13041.
Zhang, Y.M., Gao, X.L., Sun, M.L., Liu, H.Q., and Xu, J.R. (2017) The *FgSRP1* SR-protein gene is important for plant infection and pre-mRNA processing in *Fusarium graminearum*. *Environ Microbiol* **19**: 4065–4079.
Zheng, D.W., Zhang, S.J., Zhou, X.Y., Wang, C.F., Xiang, P., Zheng, Q., *et al*. (2012) The *FgHOG1* pathway regulates hyphal growth, stress responses, and plant infection in *Fusarium graminearum*. *PLoS One* **7**: e49495.
Zhou, X., Zhang, H., Li, G., Shaw, B., and Xu, J.-R. (2012) The Cyclase-associated protein Cap1 is important for proper regulation of infection-related morphogenesis in *Magnaporthe oryzae*. *PLoS Pathog* **8**: e1002911.
Zhou, X.Y., Heyer, C., Choi, Y.E., Mehrabi, R., and Xu, J.R. (2010) The *CID1* cyclin C-like gene is important for plant infection in *Fusarium graminearum*. *Fungal Genet Biol* **47**: 143–151.

Supporting Information

Additional Supporting Information may be found in the online version of this article at the publisher's web-site:

Fig. S1. Yeast two hybrid assays for the interaction of FgAma1 with FgPal1.

Yeast cells of transformants expressing the FgPal1 prey and/or FgAma1 bait constructs were assayed for growth on control SD-Leu-Trp-His (left) and β-galactosidase activities (right). The positive and negative controls were from the HybriZAP kit.

Fig. S2. Localization of FgSpa2-GFP to the hyphal tip.

Hyphal tips of transformants of the wild type (PH-1) and *Fgpal1* mutant expressing the *FgSPA2*-GFP fusion construct were examined by epifluorescence microscopy. Bar = 20 μm.

Fig. S3. Localization of FgPal1 to the hyphal tips and septa in the *Fgpom1* and *Fgkin1* mutant.

Freshly harvested germlings of the *Fgkin1*/*FgPAL1*-GFP and *Fgpom1*/*FgPAL1*-GFP transformants were examined by DIC and epifluorescence microscopy. Bar = 20 μm.

Table S1. The primers used in this study